

Fabrication of solar cells from polymer composite (3-Hexylthiophene-co-Thiophene) with Ag nanoparticles and study of electrical properties and efficiency

Ahmed Ismael^{1*}, Hussein F. Hussein², Salah S. Al-luaibi^{3*}

^{1,2}Physics Department, College of Education for Pure Sciences, Basrah University, Basrah, Iraq; ahmed.nano86@gmail.com (A.I) Husseinfalaih2020@gmail.com (F.F.H)

³Chemistry Department, College of Science, Basrah University, Basrah, Iraq; salahshakir502@gmail.com (S.S.A.I).

Abstract: This study aims to prepare nano-polymer materials that contribute to improving the electrical properties and improving the properties and efficiency of solar cells. Also, the prepared materials are inexpensive compared to solar cells prepared from inorganic materials such as silicon and germanium. This study deals with the effect of a polymer layer containing pure polymer of 3-Hexylthiophene and Thiophene in combination with silver nanoparticles on the electrical properties relevant to solar cell applications. The polymer of 3-Hexylthiophene and Thiophene was prepared individually, then a polymer composite (3-Hexylthiophene-co-Thiophene) was made. After that then a Core-Shell of (3-hexylthiophene - CO-Thiophene) @ Ag Nanoparticles was made, after which two-layer and three-layer solar cells were made from the prepared samples. The polymers were manufactured using the additive polymerization method using chloroform (CHCl₃) solvent and were subsequently characterized. The research focused on the electrical properties of the pure polymer (P3HT@Thio) doped with silver nanoparticles and its efficiency, with special attention to its application in solar cells. We found the best results in the two-layer structure. Current-voltage (I-V) measurements were conducted under illumination at room temperature with varying incident light intensities over a small area. Key parameters such as electrical conductivity, activation energy, open-circuit voltage (V_{oc}), short-circuit current density (J_{sc}), maximum power point parameters (J_p, V_p), fill factor (FF), and power conversion efficiency (η) were calculated for all samples under standard laboratory conditions. The results demonstrate that the highest electrical conductivity ($2.39 \times 10^{-3} \text{ s.cm}^{-1}$) was achieved with the polymer blend of 70% P3HT-CO-30% PTH doped with 25% silver nanoparticles (Ag NPs). The activation energy, ranging from 0.1448 eV to 0.8537 eV, showed the lowest value at the same polymer blend, likely due to the proximity of the conduction and valence band levels induced by nanoparticle doping. Additionally, the efficiency of the solar cells was assessed, revealing significant improvements in device performance. The optimal efficiency, measured at 10.488%, was observed in the (PEDOT)/(PCPM+Active Layer) structure. All relevant parameters, including J_{sc}, V_{oc}, FF, and power conversion efficiency (PCE).

Keywords: Efficiency, Electrical properties, Nano particles, Polymerization method, Poly (3HT -Co-Thio) @Ag NPs.

1. Introduction

In the past decade, photovoltaics have become a major contributor to the ongoing energy transition. Advances relating to materials and manufacturing methods have had a significant role in that development. However, there are still numerous challenges before photovoltaics can provide cleaner and low-cost energy [1].

Recently, inorganic and hybrid light absorbers such as quantum dots and organometal halide perovskites have been studied and applied in fabricating thin-film photovoltaic devices because of their low cost and potential for high efficiency [2].

The primary role of a photovoltaic cell is to receive solar radiation as pure light and transform it into electrical energy in a conversion process called the photovoltaic effect. There are several technologies involved with the manufacturing process of photovoltaic cells, using material modification with different photoelectric conversion efficiencies in the cell components.

Due to the emergence of many non-conventional manufacturing methods for fabricating functioning solar cells, photovoltaic technologies can be divided into four major generations [3].

- (1) Thick crystalline films
- (2) Thin-film solar cells
- (3) Emerging technologies
- (4) Hybrid

2. Materials

In this study, various materials were used as provided by suppliers. The monomer 3-hexylthiophene, essential for light absorption, was obtained from Meryer (SHANGHAI) CHEMICAL TECHNOLOGY CO., LTD purity. Thiophene, known for its electron-donating properties and high charge mobility, was sourced from ORGANICS USA with over 99% purity. Indium tin oxide (ITO), used for its transparency and conductivity, was acquired from Ocilla (UK) with a 1.1mm surface thickness. Solvents like analytical-grade chloroform and methanol were procured from Sigma-Aldrich and Laboratory Reagent India, respectively, ensuring high purity for device fabrication, we employed silver nanoparticles (Ag NP) with a purity of 99.9% and an average particle size (APS) of 80nm, sourced from Hongwu International Group Ltd in China. Additionally, PCBM Phenyl-C61-butyric acid methyl ester (PCBM, Molecular Formula: C₇₂H₁₄O₂) is a fullerene-based molecule and, the PCBM from Ocilla (UK) (Molar mass: MW 911 g/mol and > 99 %) is used. PEDOT: PSS Poly (3, 4-ethylene dioxythiophene): Polystyrene sulfonate, this study employed PEDOT: PSS sourced from Ossila (UK), specifically the M 124-100ml variant.

3. Experimental

3.1. Synthesis of Poly (3-hexylthiophene - CO-Thiophene)

The synthesis of the 3-hexylthiophene polymer involved several sequential steps. Initially, 0.84 gm of 3-hexylthiophene was mixed with 50 ml of chloroform (CHCl₃), and this mixture was degassed with nitrogen (N₂) for approximately 5 minutes. Subsequently, 1.62 gm of iron (III) chloride (FeCl₃) was dissolved in 50 ml of CHCl₃ then dropwise added to the degassed mixture. The reaction mixture was stirred continuously for 24 hours. After the stirring period, the mixture was washed in 100 ml of methanol, causing the 3-hexylthiophene polymer to precipitate. This process successfully yielded the desired poly (3-hexylthiophene). The same procedure was used to prepare Polythiophene (PT) using thiophene monomer instead of 3- 3-hexyl thiophene monomer. Then poly (3-hexylthiophene-CO-thiophene) was prepared by the same procedure above using percentages of 70% 3-hexylthiophene and 30% thiophene.

3.2. Synthesis of Core-Shell Polymer Nanocomposites of (3-hexylthiophene - CO-Thiophene) @ Ag Nanoparticles

In this experiment, a core-shell polymer nanocomposite was prepared using 3-hexylthiophene and a combination of Ag nanoparticles. To initiate the synthesis, 0.84 grams of 3-hexylthiophene and an equivalent amount of the nanoparticles in a 1:4 ratio were combined. This mixture was then introduced to 50 milliliters of chloroform (CHCl₃) and degassed with nitrogen (N₂) for approximately 5 minutes under ultrasonic irradiation for half an hour.

Following degassing, 1.62 grams of ferric chloride (FeCl_3) and an additional 50 milliliters of CHCl_3 were added to create a slurry. The resulting mixture was stirred for a period of 24 hours. Subsequently, it was introduced to 100 milliliters of methanol to induce polymer precipitation.

3.3. Interdigitated Finger Electrodes

The polymer solution was deposited as interdigitated finger electrodes made of aluminum obtained from the United Kingdom. These electrodes are very thin and about 10 mm long. They overlap, separated by distances of up to 100 μm , as in Figure (1). The width of the interdigitated finger electrode increases at the end of each comb to facilitate the process of connecting it to the electrical measuring circuit. These interdigitated finger electrodes have been widely used recently [4] due to their ease of use because they:

- 1- Samples can be prepared in a short period in Easy.
- 2- To deposit electrodes on the polymeric membrane, you do not need devices such as a vaporizer or a sputtering device.
- 3- Avoid the process of what is called a short circuit.
- 4- These interdigitated finger electrodes can be used several times after removing the deposited layer without any effect on the overlapping interdigitated finger electrode.
- 5- These combs can withstand temperatures lower than the melting point of aluminum (660.25 $^\circ\text{C}$).

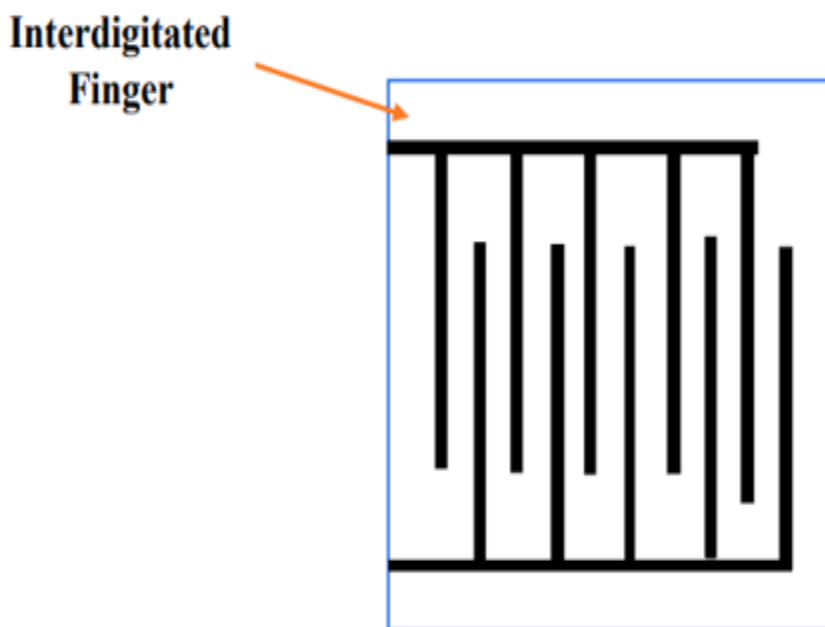


Figure 1.
Shows the shape of the interdigitated finger electrode.

The polymer solution was deposited on the interdigitated finger electrodes using a spin coater at a rotational speed, of 1500 for 20 seconds. The electrodes of the finger represent the electrodes of the circuit, and the polymer represents the layer connecting the electrodes, as shown in Figure (2).

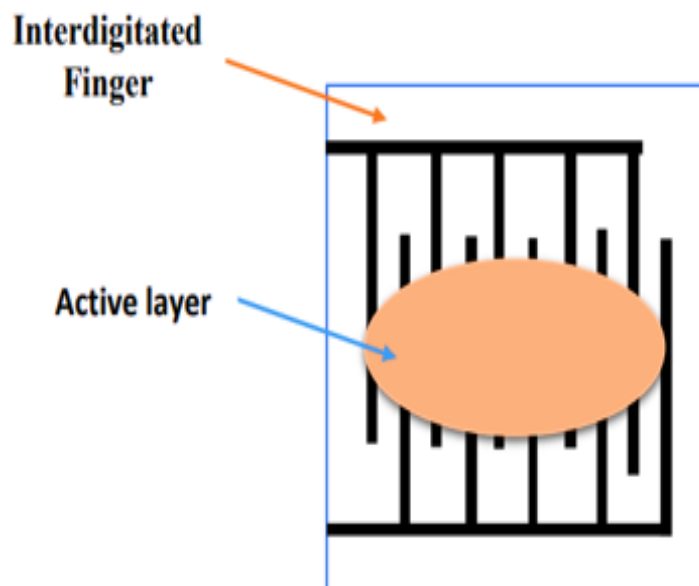


Figure 2.
The active layer deposited on interdigitated finger electrode.

4. Electrical Measurements

To study the electrical properties of the prepared films, an electrical measurement circuit consisting of a voltmeter, a power supply, and a multimeter (Digital-Multimeter - Philips). The sample to be measured is placed on a base connected to a heat source whose temperature changes (0 -70° C) and is controlled by a power supply. It contains two electrodes.

Two copper metals work in contact with the samples to be connected to the electrical measuring circuit. The parts are placed inside a wooden box closed with aluminum foil connected to copper wires connected to the ground to leak stray fields. The box also contains a small air fan to cool the sample briefly. The measuring electrical properties (current-voltage) and (current-temperature) of the prepared samples.

5. Manufacturing Devices and Measuring Efficiency

After the deposition of intermediate layers (PEDOT: PSS and PEDOT:PSS: (Poly 3-hexylthiophene-Co-thiophene) @ Ag NPs) onto the ITO-coated glass substrate, the active layer of the hybrid polymers solar cell devices is applied atop these intermediate layers. The preparation of the Poly 3-hexylthiophene-Co-thiophene) @ Ag NPs solution followed a similar procedure outlined in Section (3.2) to begin, a bilayer structure is formed by sequentially depositing the electron donor, P3HT (approximately 70 nm in thickness), and the electron acceptor, PCBM (approximately 80 nm in thickness), atop one another. This bilayer configuration forms the donor-acceptor junction, as explained in detail in Figure (3) the thicknesses of the spin-coated intermediate and blended active layers.

Where it was manufactured, all organic solar cell devices in this study followed a conventional sandwich device architecture. Four distinct solar cell devices, including hybrid polymer devices photovoltaic, were meticulously prepared and subjected to a comprehensive analysis to ascertain their characteristics. Subsequently, a thorough comparative evaluation of these nine devices was conducted, leading to the selection of those exhibiting the most favorable features for further refinement. Various device architectures have been developed to address the specific demands of efficient photon-to-charge conversion, as depicted below: Figure (3) shows four different device designs for organic solar cell cells.

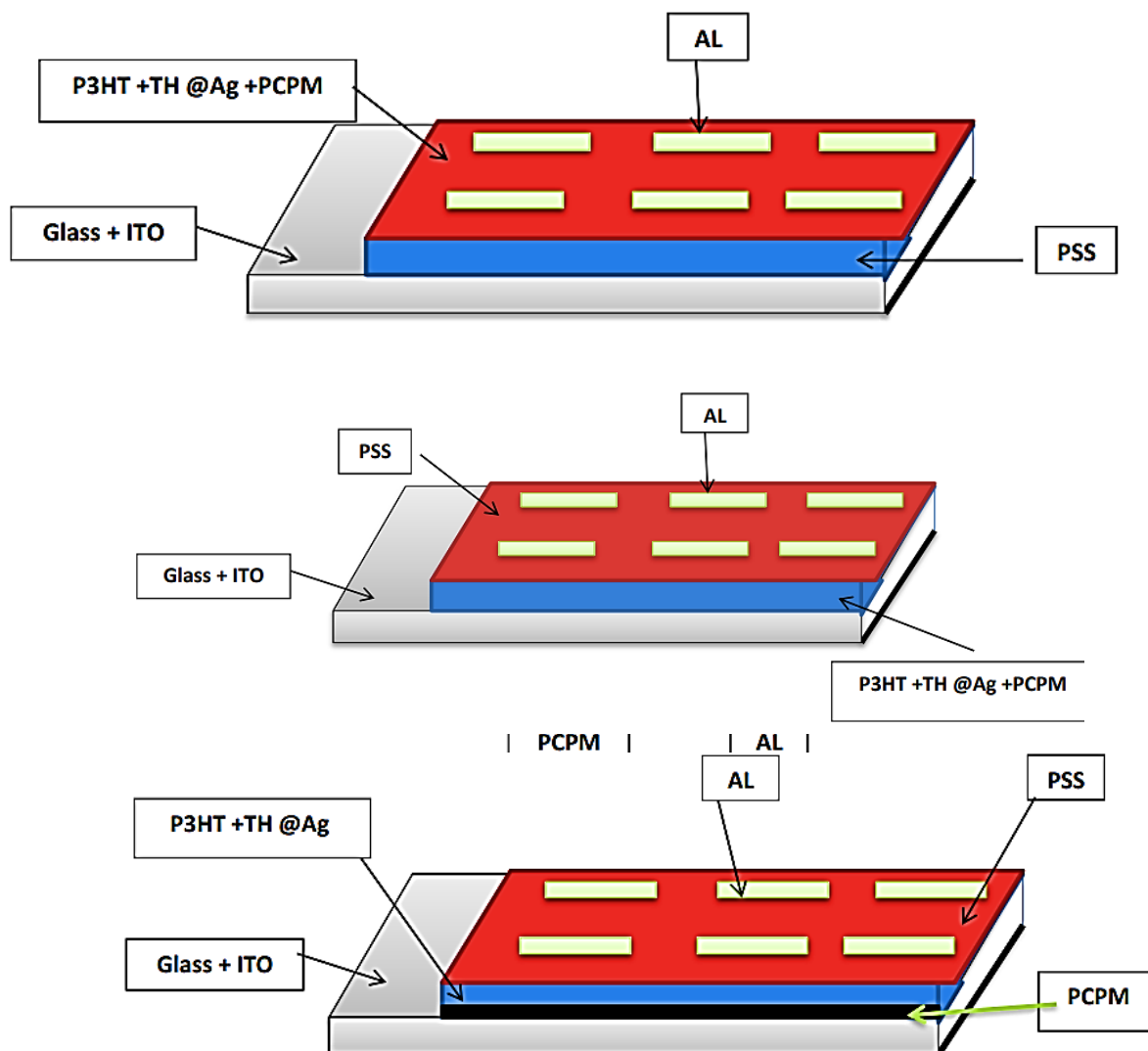


Figure 3.
Organic solar cell devises.

6. Measurement of Solar Cell Properties

The electrical circuit used in the (I-V) feature of the solar cell. The photocell measuring circuit consists of a digital current and voltage measuring device (Keithley digital Electrometer) that is connected to both ends of the sample, as well as a light source, with an input capacity of (100 mw/m^2). The sample to be chosen is fixed. It is measured on a stand at a distance of (5 cm) from the light source. The sample is connected using capillary wires and adhesive. The electrical circuit parts are connected to the computer, as shown in the following figure.

7. Results and Discussion

7.1. Current-Voltage Characteristics Measurement

The (I-V) characteristics were measured at different temperatures within the range (303 K to 330 K) as shown in Figures (4) - (8) of samples (P3HT, Poly thiophene (PT), P3HT@25% Ag NP, (70% P3HT-

CO-30%PTH), and (70% P3HT-CO-30%PTH) @ (25% Ag Np). We notice from the shapes that increasing the applied voltage leads to an increase in the current passing through the sample at all temperatures and by an increase of (5) degrees as a result of the increase in concentration and mobility of charge carriers (μ , n) when the temperature increases. All shapes share the achievement of the ohmic property at low voltages at which it was achieved. It calculated electrical conductivity from the straight-line slope in the shapes mentioned above and from the relationship (1).

Table (1) shows the electrical conductivity values with temperature. The highest conductivity values are noted. ($2.39 \times 10^{-3} \text{ s.cm}^{-1}$) were obtained with the polymer (70% P3HT-CO-30%PTH) @ (25% Ag Nanoparticles).

The increase in conductivity at this concentration is due to the increase in the number of secondary levels between the valence and conduction bands [5].

Figures (4)-(8) show the relationship between the current measured and the voltage applied to the sample's volts at temperatures (303 K-333 K) degrees Celsius. For all samples, we notice from the figures above that the current begins to increase when the voltage applied to the sample increases, as well as when the temperature increases. The increase in current may be due to the increase in charge carriers by increasing the voltage applied to the sample. While The temperature increases, it causes increased movement of molecules in the material, and the movement of charge carriers towards the conduction band increases [6].

The electric conductivity is calculated from the slope of a straight line and by equation

$$\sigma = \frac{I}{V} \left(\frac{L}{W t l} \right) \quad (1)$$

L: represents the distance between the electrodes and is equal to (100 μm).

W: represents the electrode length and is equal to (10 mm).

l: The number of electrodes deposited on the glass equals (10).

t: represents the thickness of the polymer film ($11.36 \times 10^{-5} \text{ cm}$).

$$\sigma_s = \left[\frac{I}{V t} \right] \left[\frac{100 \times 10^{-6}}{10 \times 10 \times 10^{-3}} \right]$$

$$\sigma_s = \frac{I}{V t} \left[10^{-3} \frac{\text{S}}{\text{m}} \right] \quad (2)$$

The electrical conductivity increases with temperature increase. This behavior indicates that the polymers behave as semiconductor materials [7].

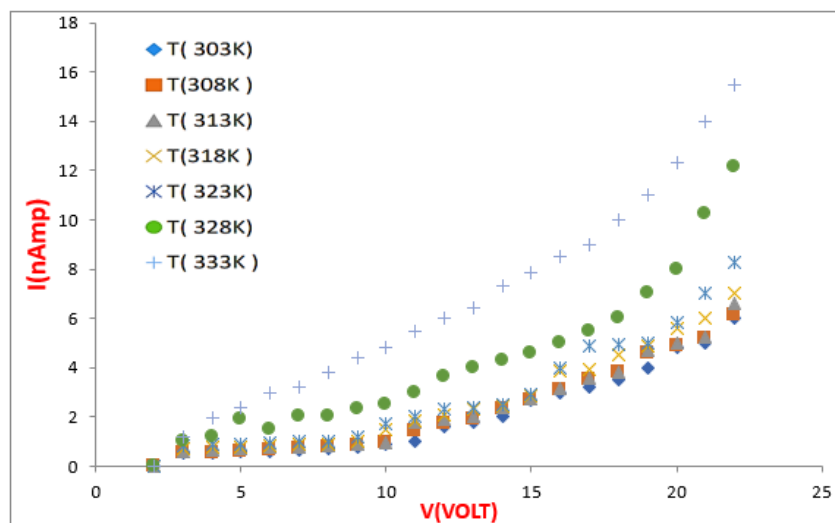


Figure 4.
(I-V) curves of P3HT

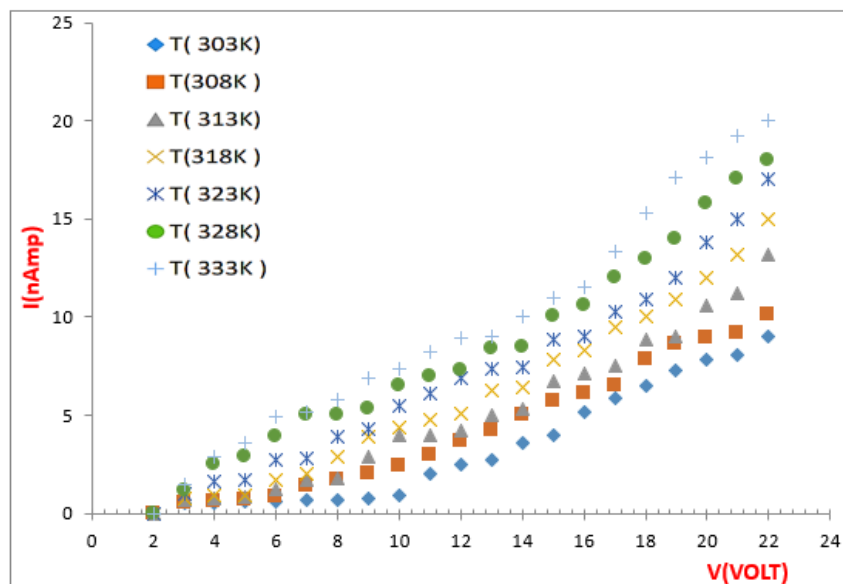


Figure 5.
(I-V) curves of Poly thiophene (PT).

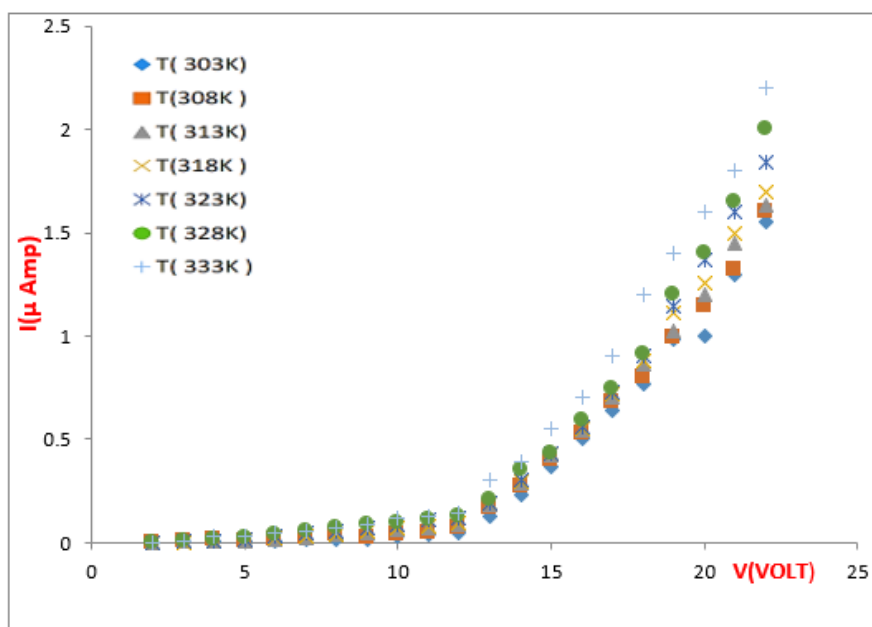


Figure 6.
(I-V) curves of P3HT@25% Ag NP.

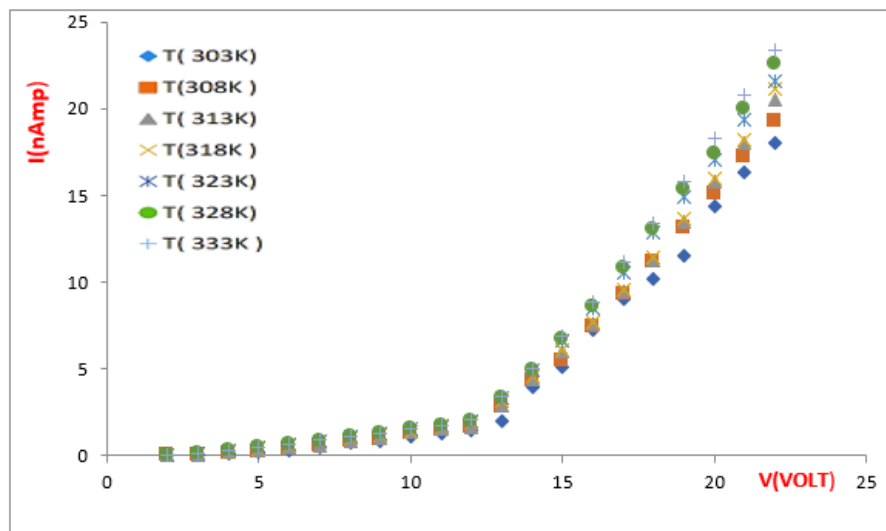


Figure 7.
(I-V) curves of (70% P3HT-CO-30%PTH).

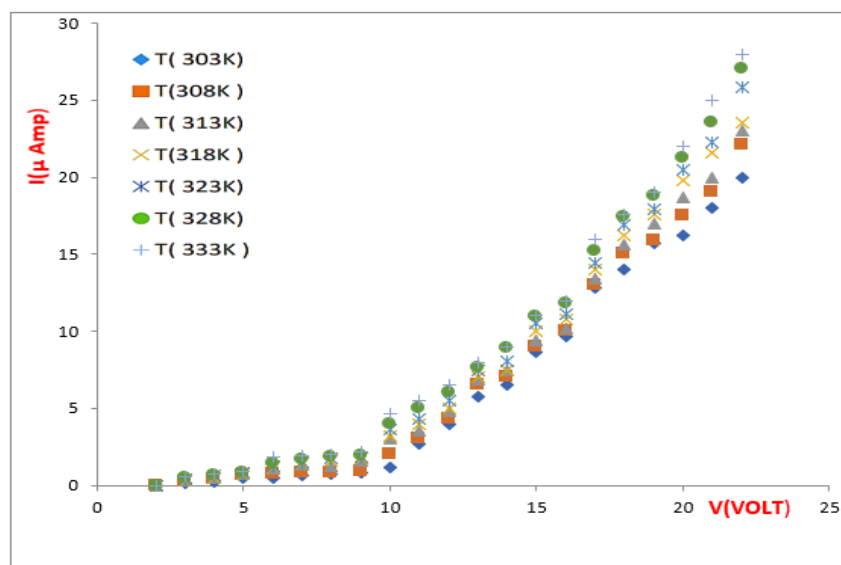


Figure 8.
(I-V) curves of (70% P3HT-CO-30%PTH) @ (25% Ag Np).

Table 1.
Shows the electric conductivity of different polymers.

Samples	$\sigma(\text{s.cm}^{-1})$
P3HT	2.51×10^{-8}
Poly thiophene (PT)	4.47×10^{-8}
P3HT@25% Ag NP	3.68×10^{-6}
(70% P3HT-CO-30%PTH)	4.48×10^{-4}
(70% P3HT-CO-30%PTH) @ (25% Ag Np)	2.39×10^{-3}

7.2. Activation Energy Results

The relationship between Lin conductivity and the inverse of the Reciprocal of temperature is shown in Figure (9) - (13) of samples (P3HT, Poly thiophene (PT), P3HT@25% Ag NP, (70% P3HT-CO-30%PTH), and (70% P3HT-CO-30%PTH) @ (25% Ag Np).

The activation energy was obtained from the slope of a straight line for the figures above and the equation

$$\sigma \dots\dots\dots (3) = \sigma_0 e^{-\frac{E_a}{kT}}$$

Where σ_0 is the term that precedes the per-exponential factor, which expresses the lowest value of electrical conductivity at absolute zero.

E_a : activation energy.

k : Boltzmann constant and its value equals (8.625×10^{-5} eV).

T : sample temperature.

The activation energy was calculated from the slope of the straight line between the conductivity and the temperature reciprocal.

Which ranges from (0.1448 eV) to (0.853748 eV) and is shown in the table(2).

We note from Table (2) that the lowest activation energy value was (0.1448 eV) of the sample (70% P3HT-CO-30%PTH) @ (25% Ag Np) due to the proximity of the conduction and valence band levels as a result of doping with nanoparticles (Ag Np). The activation energy of a polymer (70% P3HT-CO-30%PTH) @ (25% Ag Np) decreases with increasing temperature due to the increase in the kinetic energy of the polymer molecules.

This increase in kinetic energy allows the molecules to overcome the activation energy barrier more quickly, increasing the reaction rate.

The increase in temperature can also cause the polymer chains to become more disordered, decreasing the activation energy [8].

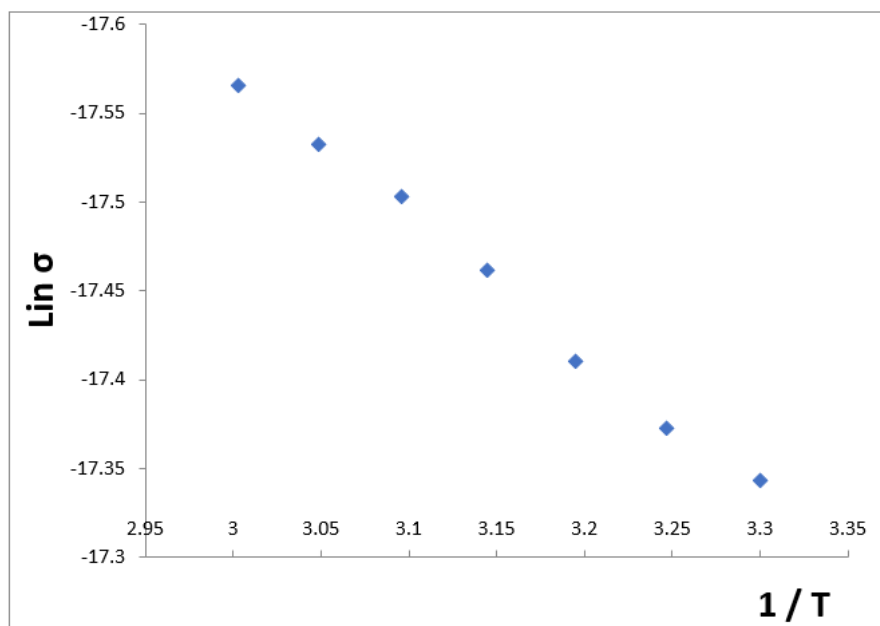


Figure 9.
($\text{Ln } \sigma - \frac{1}{T}$) curves of P3HT.

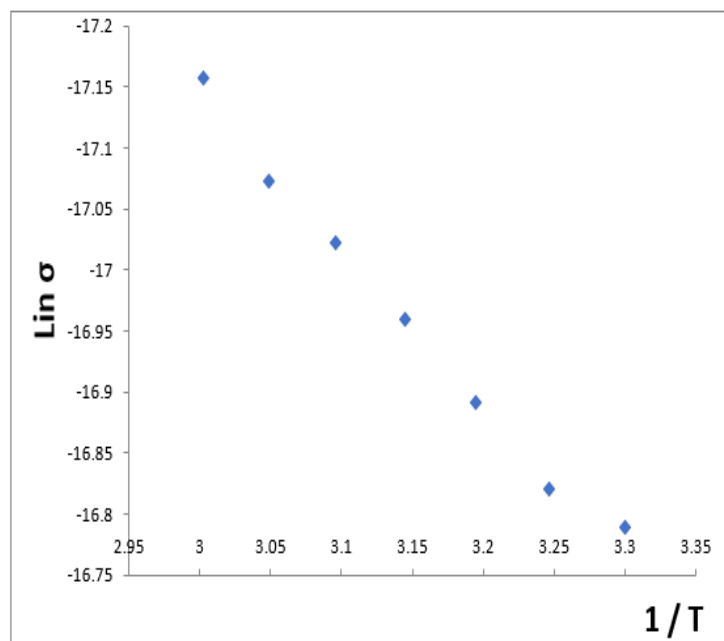


Figure 10.
 ($\text{Ln } \sigma - \frac{1}{T}$) curves of Poly thiophene (PT).

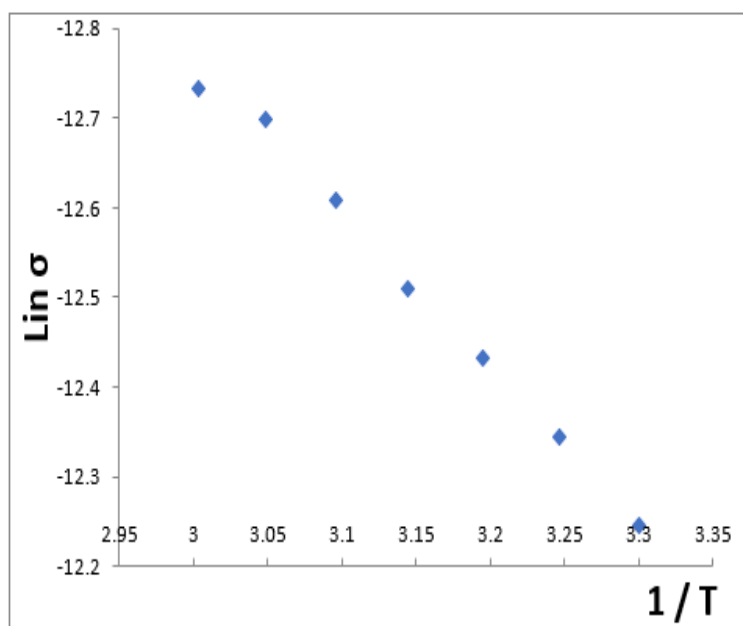


Figure 11.
 ($\text{Ln } \sigma - \frac{1}{T}$) curves of P3HT@25% Ag NP.

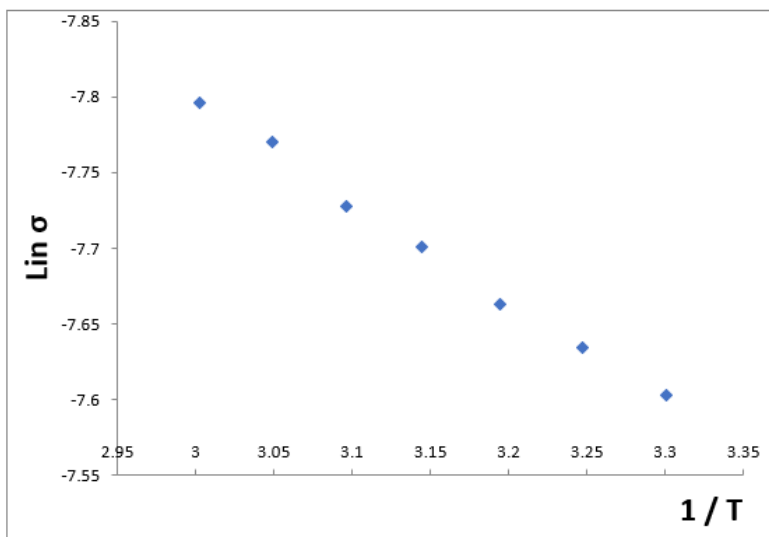


Figure 12.
($\text{Ln } \sigma - \frac{1}{T}$) curves of (70% P3HT-CO-30%PTH).

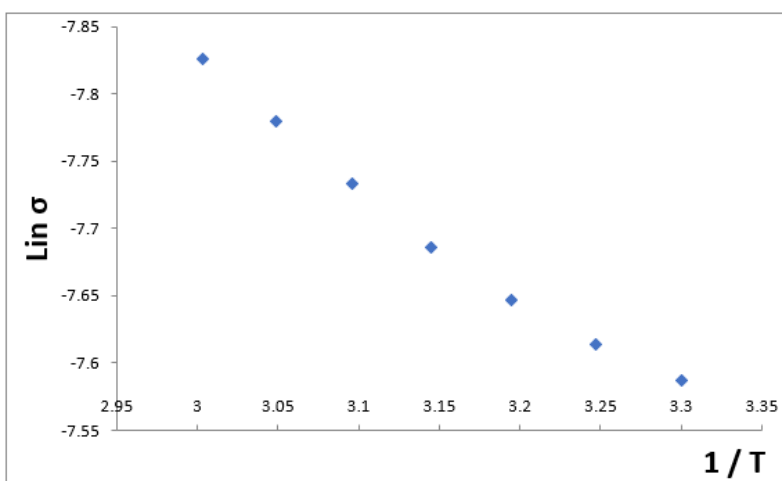


Figure 13.
($\text{Ln } \sigma - \frac{1}{T}$) curves of (70% P3HT-CO-30%PTH) @ (25% Ag NP).

Table 2.
Shows activation energy for different polymers.

Samples	E_a (eV)
P3HT	0.6177
Poly thiophene (PT)	0.7135
P3HT@25% Ag NP	0.853747
(70% P3HT-CO-30%PTH)	0.382
(70% P3HT-CO-30%PTH) @ (25% Ag NP)	0.1448

7.3. Samples Histogram of Activation Energy

The graph shown in Figure (14) was drawn, which shows the calculated activation energy, which is the initial energy needed by electric charges to move within the material. E_a increases with temperature in insulators and semiconductors and decreases in metals. As E_a increases, more energy is needed to move the charges within the structure. However, in our research, the activation energy values of the prepared polymers, namely **(70% P3HT-CO-30%PTH) @ (25% Ag NP)** The lowest activation energy value was observed (0.1448). This is due to the addition of nanoparticles, which caused a significant increase in electrical conductivity and decreased activation energy. This decrease in activation energy makes it easier for charges to flow, thus enhancing the overall electrical properties of the material; these results are better than the results for samples prepared previously in research [9,10].

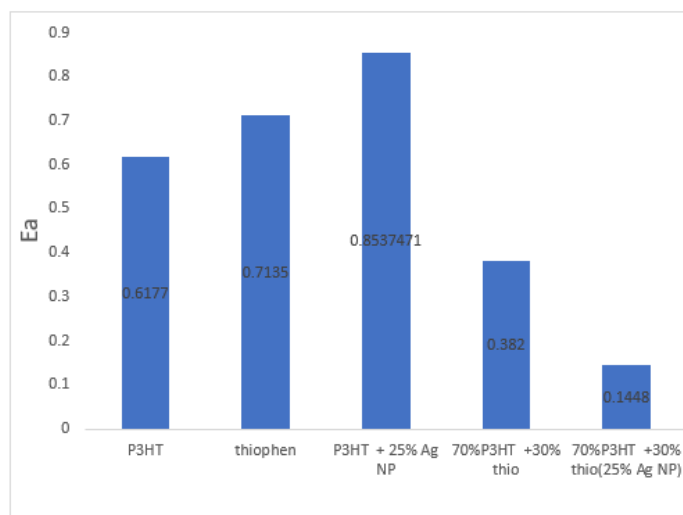


Figure 14.
Shows a histogram of activation energy for different samples.

7.4. Current – Voltage Characterization of Solar Cell Devices

Characterizations (J-V) of four different Solar cell devices given were obtained under simulated illumination intensity of solar light (100 mw/cm^2) at room temperature. Their solar cell parameters from current voltage data are given in Table (3).

Data are extracted from each cell group and the respective standard deviations are calculated.

The current intensity of the current data was calculated through the equation

$$\text{The current intensity (J)} = \frac{\text{Current (I)}}{\text{Effective layer area(A)}} \quad (4)$$

By drawing a graph between voltage and current intensity, each of the parameters was calculated (V_{oc} , J_{sc} , J_p , V_p , FF, η According to equations

$$V_{oc} = \frac{1}{e} (E_{\text{HOMO-donor}} - E_{\text{LUMO-acceptor}}) + C \quad (5)$$

Where C is an empirical constant that is concerned with the dark I-V curve of the diode

$$FF = \frac{P_{max}}{V_{oc} I_{sc}} = \frac{V_{max} I_{max}}{V_{oc} I_{sc}} \quad (6)$$

V_{max} and I_{max} are the voltage and current at the maximum output power [129].

$$\text{PCE } \eta = \frac{P_{out}}{P_{IN}} = \frac{V_{oc} I_{sc} FF}{P_{IN}} \quad (7)$$

P_{IN} is the input power under Standard Test Condition (100 w/cm², AM 1.5 (Air Mass) solar spectrums, temperature during measurements 30°C [11]).

7.5. Current density–Voltage (J–V) Characterization

Figures (15) - (18) show the J–V curve of the samples PCPM / Active Layer/ PEDOT: PSS, PEDOT: PSS /Active Layer / PCBM, (Active layer +PCPM) / (PEDOT: PSS), (PEDOT: PSS)/(PCPM+Active Layer). A reasonable photovoltaic effect was observed with short-circuit current density (J_{sc}), open-circuit voltage (V_{oc}), fill factor (FF), and power conversion efficiency (PCE) Calculated from the two equations (4, 5, 6, and 7) respectively for all structures shown in Table (3). The slight increase in the PCE value is due to the middle layer PEDOT: PSS, which has high transparency in the visible range and is useful for use as an anode buffer layer in organic solar cells, which is a better result than the result (2.16%) recorded in the research [188]. It is also due to PSS having linear electrical conductivity with large absorption of gravitational charge and electrostatic shielding facilitated by the presence of sulfide groups. In addition, the light absorption properties increased with increasing wavelengths of incident light, with a strong absorption peak at 220–225 nm higher than PCPM [12]. The increase in the efficiency of the third and fourth compositions is due to mixing the nanoparticles with PCPM, which alleviates the thermal phase transition problem and leads to improving the energy conversion efficiency and the overall stability of solar cells. It is a high-potential material for application in lead perovskite solar cells due to its low cost, high photoactivity, and exceptional stability [13].

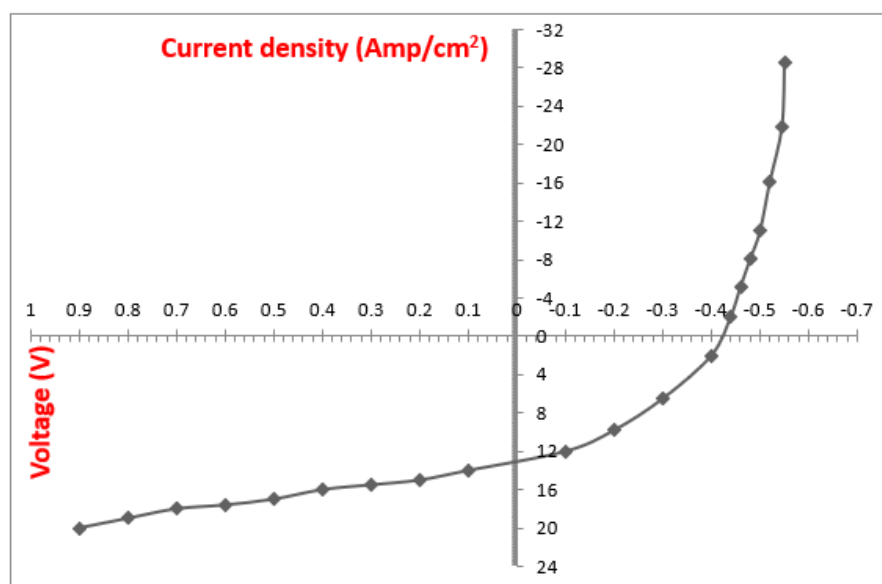


Figure 15. (J–V) curves of (70% P3HT-CO-30%PTH) @(25% Ag Np)solar cell devise.

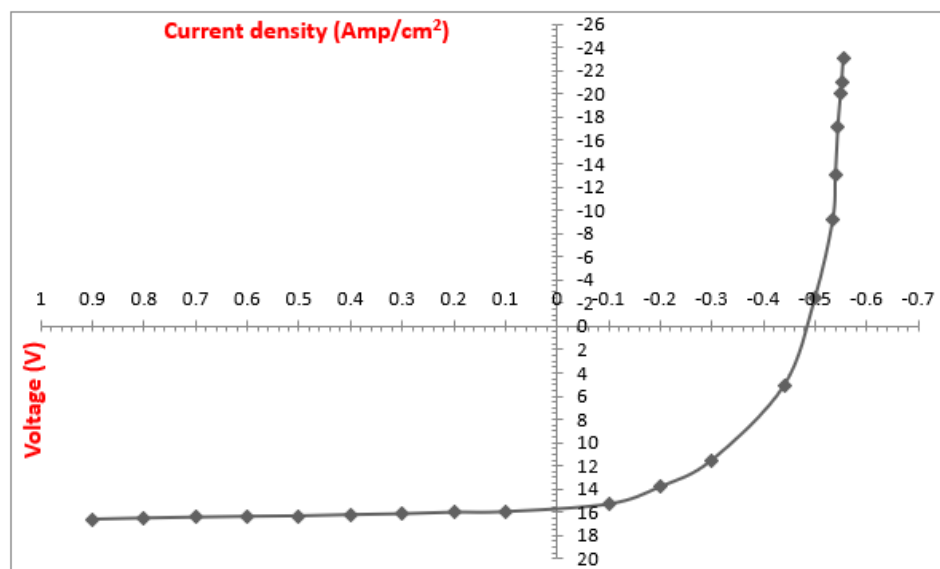


Figure 16.
(J-V) curves of PEDOT: (70% P3HT-CO-30%PTH) @ (25% Ag Np)/PCBM for solar cell device.

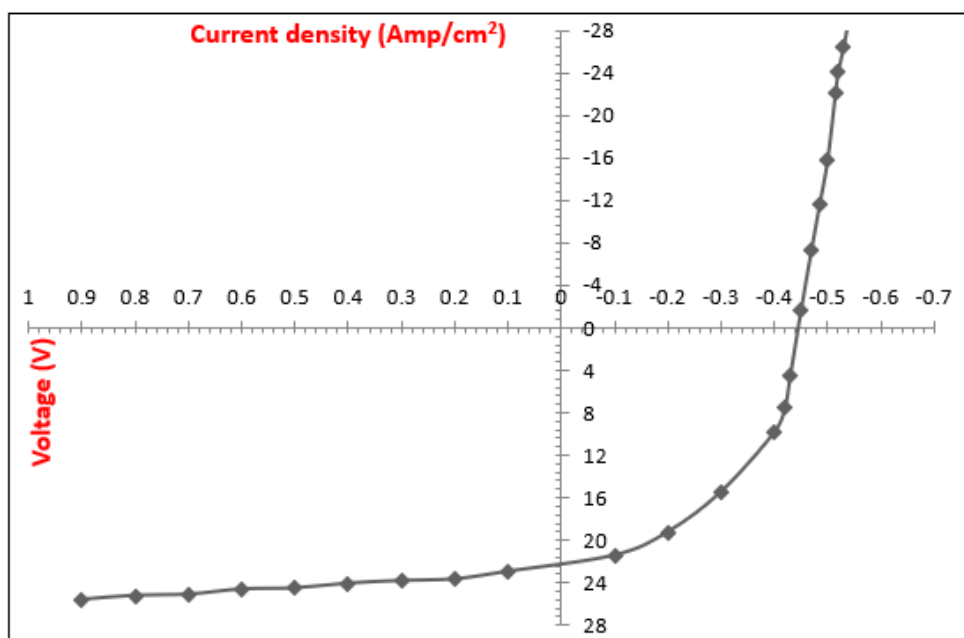


Figure 17.
(J-V) curves ((70% P3HT-CO-30%PTH) @ (25% Ag Np) + PCPM) / (PEDOT: PSS) for solar cell device.

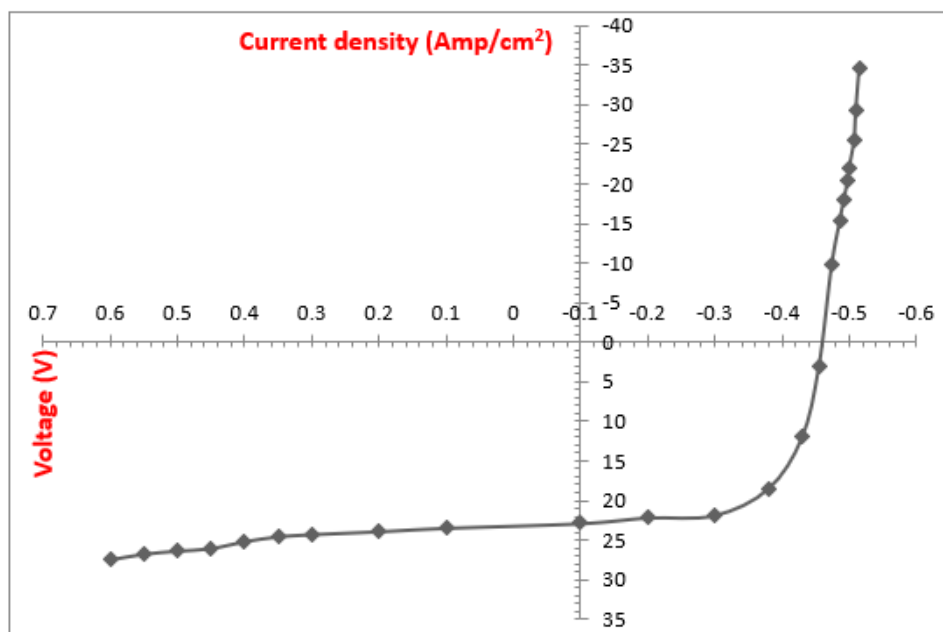


Figure 18.
(J-V) curves of (PEDOT: PSS)/(PCPM+((70% P3HT-CO-30%PTH)@(2.5% Ag Np)) for solar cell device.

Table 3.

The table represents a summary of the samples.

Sample	Voc	Jsc	Vax	Jmax	Pmax	FF	η
PCPM / Active Layer/ PEDOT: PSS	0.26	8	0.42	13	5.46	2.625	5.46
PEDOT: PSS /Active Layer / PCBM	0.322	10.5	0.48	15.7	7.536	2.22893	7.536
(Active layer +PCPM) / (PEDOT: PSS)	0.308	15.4	0.44	22	9.68	2.04082	9.68
(PEDOT: PSS)/ (PCPM+Active Layer)	0.385	18.5	0.46	22.8	10.488	1.47252	10.488

8. Effect of Exposure Time on the Efficiency of Solar Cell Devices

The present study exposed samples to air for (twelve weeks) at room temperature. Figures (19) show the power conversion efficiency versus the exposure time in the air for samples including structures PCPM/ Active layer/PEDOT: PSS, PEDOT: PSS /Active Layer /PCBM, (Active layer +PCPM) / (PEDOT: PSS), and (PEDOT: PSS)/(Active layer+PCPM). The active layer here includes the copolymer and nanoparticles Ag.

The efficiency value reaches a maximum value after (week), then slowly decreases after (Two weeks). The film was sensitive to the oxygen in the air and the hence produced films are particularly unstable. Therefore, careful encapsulation and handling in the arid and oxygen-free atmosphere may reduce the instability and keep the electrical and photovoltaic properties for the long term.

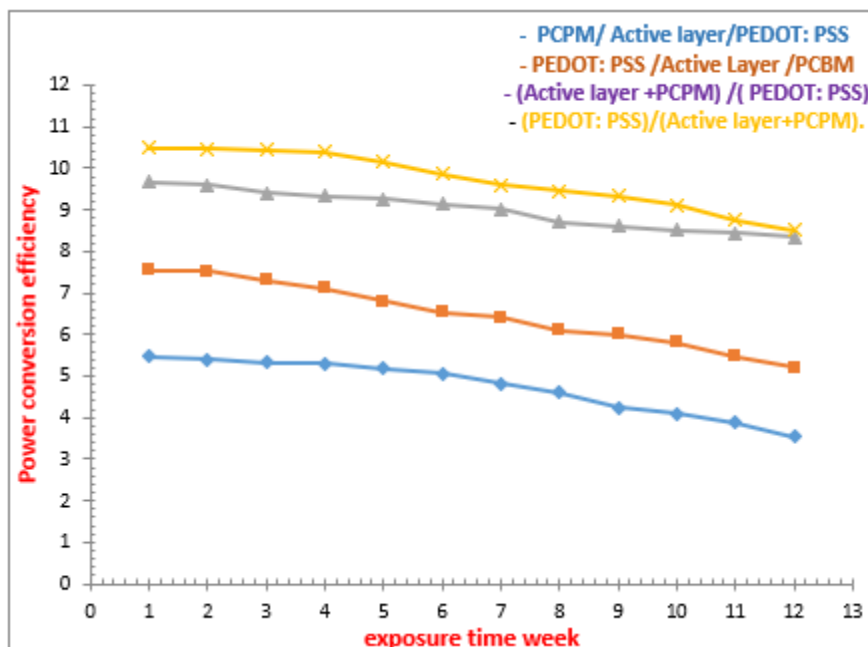


Figure 19. Efficiency with an exposure time of (PEDOT: PSS)/ ((70% P3HT-CO-30%PTH) @ (25% Ag Np) + PCPM) for solar cell devices.

9. Conclusion

In this comprehensive study, we meticulously prepared polythiophene (PT), poly-3-hexylthiophene (P3HT), and their copolymer Poly (3HT-Co-PT) using free radical polymerization. Our careful approach ensures the reliability and thoroughness of our findings. Additionally, we crafted several hybrid polymers using (Core - Shell) Polymerization in the presence of Nano-silver, at a percentage of 25%.

The diverse array of samples we prepared in different proportions, demonstrates the breadth and depth of our study.

- 1- Poly3-hexyl thiophene (P3HT)
- 2- Poly thiophene (PT)
- 3- P3HT@25% Ag NP
- 4- (70% P3HT-CO-30%PTH)
- 5- (70% P3HT-CO-30%PTH) @ (25% Ag Np)

The electrical properties of the prepared films were studied, as the feature (current-voltage) and continuous electrical conductivity with temperature were studied, reaching their highest value for the polymer.

(70% P3HT-CO-30%PTH) @ (25% Ag NP), about ($2.39 \times 10^{-3} \text{ s.cm}^{-1}$). It has been observed graphically that electrical conductivity increases with increasing temperature for all prepared samples, from which we conclude that these prepared materials have a positive thermal conductivity coefficient, as they act as semiconductors that can be used in electronic applications, including solar cells. The activation energy of the prepared films was calculated.

Hybrid solar cells were manufactured by depositing the prepared polymer solution onto (ITO-glass) bases using the spin coating technique and depositing electrodes using a vacuum pressure evaporator (10-5). Where (4) models with the structure were prepared

- 1- [ITO/ PEDO: PSS / P3HT@PT (25%Ag) / PCBM] AL

- 2- [ITO/ PCBM/ P3HT@PT (25%Ag) / PEDO: PSS] AL
 3- [ITO/P3HT@PT (25%Ag) +PCBM/ PEDO: PSS] AL
 4- [ITO/ PEDO: PSS/P3HT@PT (25%Ag) +PCBM] AL

It was found that organic solar cells perform best when gold nanoparticles are added to the copolymer with PCBM as one layer and PEDO: PSS as the second layer. The results showed that the best solar cell efficiency value is for the cell ITO/PEDO: PSS/P3HT@PT (25% Ag) + PCBM (10.488%).

The apparent improvement in the efficiency of the solar cell can be mainly attributed to the increase in the value of the short-circuit current density (J_{sc}), in which the active layer (P3HT@PT (25%Ag) +PCBM) has the most excellent length for the diffusion of excitons (electron-hole).

Copyright:

© 2024 by the authors. This article is an open access article distributed under the terms and conditions of the Creative Commons Attribution (CC BY) license (<https://creativecommons.org/licenses/by/4.0/>).

References

- [1] L. Tsakalakos, "Introduction to Photovoltaic Physics, Applications, and Technologies," in *Nanotechnology for Photovoltaics*, USA, Taylor & Francis eBooks, 2010, p. 48.
- [2] W. Z. S. D. S. S. W. J. Snaith*†, "Enhancement of Perovskite-Based Solar Cells Employing Core-Shell Metal Nanoparticles," *ACS Publications*, vol. Vol 13/Issue 9, no. 4505-4510, August 15, 2013. <https://doi.org/10.1021/nl4024287>.
- [3] A. D. J. S. C. G. Samy Almosni, "Material challenges for solar cells in the twenty-first century: directions in emerging technologies," *Science and Technology of Advanced Materials*, vol. 19, no. 1, 2018 . <https://doi.org/10.1080/14686996.2018.1433439>.
- [4] S.S. Ebade, "Studying of Adhesion Force and Electrical Properties of Poly (Aniline -Co-Ally Alcohol) films deposited on different Substrates, College of Education of pure science, MSC.thesis, (2014). ; <https://doi.org/10.3390/polym12061397>
- [5] N. K. a. b, "Elucidation of the highest valence band and lowest conduction band shifts using XPS for ZnO and Zn0.99Cu0.01O band gap changes," *ScienceDirect*, vol. 6, no. 1183-1190, pp. 217-230, 2016. <https://doi.org/10.1016/j.rinp.2016.04.001>
- [6] Thomas, G. A., et al. "Temperature-dependent conductivity of metallic doped semiconductors." *Physical Review B* 26.4 (1982): 2113. DOI:<https://doi.org/10.1103/PhysRevB.26.2113>
- [7] Hussein, H. F., W. Abdul Ghafor, and A. M. Hadad. "Electric properties of carbon black filled benzidine terminated poly (pamino benzaldehyde) films." *Iraqi J. Polymer* 4.1 (2000): 59-68.
- [8] Vyazovkin, Sergey. "Activation energies and temperature dependencies of the rates of crystallization and melting of polymers." *Polymers* 12.5 (2020): 1070. <https://doi.org/10.3390/polym12051070>
- [9] Olayo, Ma Guadalupe, et al. "Conductivity and activation energy in polymers synthesized by plasmas of thiophene." *Journal of the Mexican Chemical Society* 54.1 (2010): 18-23.
- [10] Obrzut, Jan, and Kirt A. Page. "Electrical conductivity and relaxation in poly (3-hexylthiophene)." *Physical Review B— Condensed Matter and Materials Physics* 80.19 (2009): 195211.
- [11] A. Luque and S. Hegedus, *Handbook of photovoltaic science and engineering*. Wiley. Com, 2011.
- [12] Favaloro, Michael. Properties and processes of linear polyphenylene sulfide (PPS) for continuous fiber composites aerospace applications. No. 2009-01-3242. SAE Technical Paper, 2009. DOI: <https://doi.org/10.4271/2009-01-3242>
- [13] Cochran, J. Kirk, Henry J. Bokuniewicz, and Patricia L. Yager. *Encyclopedia of ocean sciences*. Academic Press, 2019.